

Autophagy is increased in cryptorchid testis resulting in abnormal spermatozoa

Marina G Yefimova, Antoine Buschiazzo, Agnes Burel, Marie-Thérèse Lavault, Celine Pimentel, Guilhem Jouve, Sylvie Jaillard, Bernard Jegou, Nicolas Bourmeyster, Célia Ravel

▶ **To cite this version:**

Marina G Yefimova, Antoine Buschiazzo, Agnes Burel, Marie-Thérèse Lavault, Celine Pimentel, et al.. Autophagy is increased in cryptorchid testis resulting in abnormal spermatozoa. Asian Journal of Andrology, 2019, 21 (6), pp.570. 10.4103/aja.aja_12_19 . hal-02119174

HAL Id: hal-02119174
https://univ-rennes.hal.science/hal-02119174

Submitted on 9 Jul 2020

HAL is a multi-disciplinary open access archive for the deposit and dissemination of scientific research documents, whether they are published or not. The documents may come from teaching and research institutions in France or abroad, or from public or private research centers.

L'archive ouverte pluridisciplinaire **HAL**, est destinée au dépôt et à la diffusion de documents scientifiques de niveau recherche, publiés ou non, émanant des établissements d'enseignement et de recherche français ou étrangers, des laboratoires publics ou privés.

[Downloaded free from http://www.ajandrology.com on Thursday, July 9, 2020, IP: 92.167.220.122]

Asian Journal of Andrology (2019) 21, 570–576
www.asiaandro.com; www.ajandrology.com

Open Access

ORIGINAL ARTICLE

Sperm Biology

Autophagy is increased in cryptorchid testis resulting in abnormal spermatozoa

Marina G Yefimova[1,2], Antoine Buschiazzo[1], Agnes Burel[3], Marie-Therese Lavault[3], Celine Pimentel[4], Guilhem Jouve[1], Sylvie Jaillard[5], Bernard Jegou[6], Nicolas Bourmeyster[7], Celia Ravel[1]

Autophagy is involved in spermatogenesis by regulating germ cell maturation. This catabolic process increases with hyperthermic conditions to prevent the accumulation of damaged organelles. Cryptorchidism is associated with impairment of germ cell maturation revealed by the presence of immature forms of sperm cells in ejaculates. The aim of the present study was to evaluate the status of autophagy in sperm cells from cryptorchid patients. Semen samples of cryptorchid patients and normozoospermic controls were analyzed by immunocytochemistry and electron microscopy. Autophagy proteins, autophagy-related protein 9 (ATG9) and microtubule-associated protein, 1A/1B-light chain 3 (LC3) were localized by immunocytochemistry on the acrosome and on the equatorial segment of sperm cells. LC3 was also detected in the midpiece of cryptorchid sperm tail. Autophagy substrate p62 protein was present in the acrosome and in the postequatorial segment of sperm in control samples, but not in the cryptorchid ones. Transmission electron microscopy revealed double-membrane-limited autophagosomes in postequatorial part of spermatozoa head and midpiece in cryptorchid samples. Partly degraded mitochondria were frequently discerned in autophagic vacuoles. In conclusion, autophagy is increased in sperm cells from patients with cryptorchid history comparatively to control. Our work provides insights into the role of autophagy in the maturation and survival of human male gametes in pathological conditions. Thus, regulating autophagy could represent a potential way to improve sperm quality in cryptorchid men.

Asian Journal of Andrology (2019) **21**, 570–576; doi: 10.4103/aja.aja_12_19; published online: 24 April 2019

Keywords: autophagy; cryptorchidism; mitophagy; spermatozoa

INTRODUCTION

Cryptorchidism or maldescended testes is the most common developmental abnormality, with the incidence of 2%–8% in full-term boys and 30%–33% in premature boys.[1] Factors influencing testicular descend are grouped as genetic, hormonal and environmental, or their combination.[2] Cryptorchidism is associated with impaired spermatogenesis.[3,4] Abnormal intra-abdominal environment of cryptorchid testes and exposition to elevated temperature strongly affect both germ and somatic cells, which display dramatic changes in morphology, function, and gene expression.[5] Aberrant structure of Leydig cells,[6,7] vacuolization of Sertoli cell, abnormal cell adhesion and disruption of Sertoli-cell supported blood-testis barrier are the consequences of cryptorchidism in human[6,8,9] and animal experimental models.[7,10,11] Besides, epididymal anomalies are often associated with the undescended testis.[12,13]

Cryptorchidism is recognized as one of the strongest risk factors for infertility in adulthood,[14–16] as confirmed by experimental and epidemiologic studies.[5] While the surgical correction of cryptorchidism (orchidopexy) in children is considered as an efficient mode of treatment, both structural and functional alterations are detected in the testes with a history of cryptorchidism.[14] The decrease of semen quality (sperm cell number, motility, and sperm cell malformations), and the presence of immature forms of spermatozoa with uncondensed nuclei, aberrant acrosomes, and large cytoplasmic residues have been reported in men who underwent orchidopexy for cryptorchidism during childhood.[15–17] Serum hormones level also deviates from normal values so an increase of follicle-stimulating and luteinizing hormones or a decrease of inhibin was, for example, detected in men subjected to orchidopexy in the childhood.[18]

Autophagy is a catabolic pathway which takes place in all eukaryotic cells. It provides the transport of nonessential, old or damaged components to lysosomes for lysosome-mediated degradation and turnover process.[19] Autophagic degradation of damaged mitochondria (mitophagy) is a sort of selective autophagy. It plays critical roles in fundamental biological processes such as terminal differentiation of red blood cells and paternal mitochondrial degradation, as well as in pathological states, including some neurodegenerative diseases, ischemia or drug-induced tissue injury.[20] In contrast to apoptosis, which is a programmed cell death,[21] autophagy is primarily a cell survival process, which intervenes under various conditions of cellular

[1]Univ Rennes, CHU Rennes, Laboratoire de Biologie de la Reproduction -CECOS, Inserm, EHESP, Irset (Institut de recherche en santé, environnement et travail) - UMR_S 1085,Rennes F-35000, France; [2]Sechenov Institute of Evolutionary Physiology and Biochemistry, Russian Academy of Sciences, 194223 St-Petersburg, Russia; [3]Univ Rennes, Biosit Platform - MRIC, Rennes 35000, France; [4]Univ Rennes, CHU Rennes, Department of Gynecology Obstetric and Human Reproduction, Rennes 35000, France; [5]Univ Rennes, CHU Rennes, Department of Cytogenetic, Irset (Institute for Environmental and Occupational Health) – UMR_S 1085, Rennes 35000, France; [6]Univ Rennes, Inserm, EHESP, Irset (Institute for Environmental and Occupational Health) – UMR_S 1085, Rennes F-35000, France; [7]University of Poitiers - CHU Poitiers, STIM ERL 7003 CNRS, Poitiers 86021, France.
Correspondence: Dr. C Ravel (celia.ravel@chu-rennes.fr)
Received: 28 May 2018; Accepted: 10 January 2019

[Downloaded free from http://www.ajandrology.com on Thursday, July 9, 2020, IP: 92.167.220.122]

stress, such as starvation, hyperthermia, and different cytotoxic insults, thereby conferring adaptation to the changing environment.[19,20] Nevertheless, uncontrolled activation of autophagy can promote cell death, of which morphological appearance differs from those of apoptosis.[19,21]

Autophagy is regulated by the autophagy-related (*ATG*) genes originally identified in yeast and their mammalian homologs.[19] Being initiated, autophagy progresses through a series of consecutive steps, starting from the formation of a pre-autophagosomal membrane phagophore, its further maturation into a double-membrane-limited autophagosome, which then fuses with lysosome for degradation of sequestered cargoes. Several proteins can be used as specific markers to evaluate the progression of autophagy such as ATG9 protein at the phagophore assembly, microtubule-associated protein, 1A/1B-light chain 3 (LC3)-II protein (membrane form of LC3 protein) at the stage of elongation and formation of autophagosome or p62 protein (which is a selective autophagy substrate protein) at the final stage of autophagy.[19] Nevertheless, high-resolution transmission electron microscopy allowing to distinguish double-membrane-limited vacuoles filled with different cargoes remains the "gold standard" to assess autophagy in tissues.[22]

Autophagy has been shown to regulate germ cell maturation in animal models.[23,24] It interferes at the spermiation stage when round spermatids undergo metamorphosis process leading to the formation of the streamlined spermatozoa.[25] Conditional knockout of autophagy-related genes in mice severely affects the fertility, resulting in generation of functionally disabled spermatozoa showing the signs of immaturity (malformed and/or absent acrosome, large cytoplasmic droplet, and decreased motility[23,24]), resembling those observed in cryptorchid animals.[26–28]

Autophagy is known to be initiated in hyperthermic conditions under which it acts as the primary cytoprotective mechanism, preventing the accumulation of protein aggregates and damaging organelles formed in cells exposed to heat shock.[29] Elevated environmental temperature within the body cavity is believed to be a primary factor affecting spermatogenesis in cryptorchid testes.[30–32] While the molecular mechanisms behind this have not been fully determined, later stage haploid germ cells seem to be the most susceptible when exposed to abdominal temperature.[5] A study from experimental cryptorchid rat model revealed an involvement of autophagy in testicular spermatogenesis damage.[33]

To our knowledge, no information on autophagy status in sperm cells from patients with cryptorchid history is available to date. In this work, we aimed to evaluate the status of autophagy in spermatozoa from patients who underwent orchidopexy during childhood by immunohistochemistry and electron microscopy.

PATIENTS AND METHODS

Patients

Semen samples were obtained from the French Biobank GERMETHEQUE from 10 patients with cryptorchid history and 8 as control individuals attending the Laboratory of Reproductive Biology CECOS (University Hospital Center of Rennes, Rennes, France) for assisted reproduction technology or before vasectomy, respectively. All patients displayed a normal karyotype and neither radiotherapy history nor chemotherapy. The study was approved by the Local Ethics Committee (CE GMR 17-03 Rennes, France) and was conducted in accordance with the Helsinki II declaration and with the French law on clinical research. Informed and written consent was obtained from all individual participants included in the study.

Semen collection

Semen samples of the patients were collected by masturbation after 3–5 days of sexual abstinence and examined after liquefaction for 30 min at 37°C. Sperm volume and pH, concentration and motility of spermatozoa were evaluated according to the World Health Organization guidelines.[34]

Immunocytochemistry

Semen samples were smeared on Thermo Scientific™ SuperFrost™microscope glass slides (Z692255-100EA, Sigma-Aldrich, St. Louis, MO, USA). Samples were then fixed with 4% paraformaldehyde (PFA)/PBS (R37814, Invitrogen, Waltham, MA, USA; BE17-512F, Lonza, Basel, Switzerland) for 10 min, washed three times with PBS and dried out at room temperature for 1 h. The samples were permeabilized with 0.1% Triton X-100/PBS (T8787, Sigma-Aldrich), briefly washed and incubated overnight with primary antibodies diluted 1:250 in 1% bull serum albumin (BSA)/PBS (A9647, Sigma-Aldrich) at 4°C. All primary antibodies were rabbit polyclonal antibodies from Novus biologicals (anti ATG9 [NB110-56893], anti LC3 [NB100-2220] and anti p62 [NBP1-48320]; Centennial, CO, USA). Next day the samples were washed in PBS, and then incubated with secondary antibodies (Chicken anti-Rabbit Alexa-448, dilution 1:500 in 1% BSA/PBS; A-21441, Invitrogen), at room temperature for 1 h, washed and counterstained with 0.5 μg ml^{-1} 4,6-diaminido-2-phenylindole (DAPI, 62247, Thermo Fisher Scientific, Waltham, MA, USA). To check for the specificity of antibodies, the control experiments were carried out using the control peptides from Novus biologicals: NB110-56893PEP (for ATG9) and NB100-2220PEP (for LC3) according to the supplier's protocol. To this end, 5 μl (10 × excess) of blocking peptide was added to 250 μl of the primary antibody (dilution 1:250 in 1% BSA/PBS). The mix was incubated for 1 h at room temperature with gentle stirring, and then dropped on the slides. The slides were incubated overnight at 4°C and then processed as described above. In additional control experiments, a nonimmune rabbit serum (933B-02, MERCK, Darmstadt, Germany; dilution 1:250 in 1% BSA/PBS) was applied instead of the primary antibody. The slides were observed under an upright Nikon Eclipse NiE microscope (Nikon Instruments Europe B.V., Amstelveen, the Netherlands). The pictures were taken using an Orca–R2 C10600 camera (Hamamatsu, Hamamatsu City, Japan).

Transmission electron microscopy (TEM)

Semen samples were diluted in Ferticult IVF medium (FECV050, Fertipro, Beernem, Belgium) 1:5 (*v*/*v*), then centrifuged at 600*g* for 10 min (Heraeus Multifuge X1R Centrifuge 75004250, Thermo Fisher Scientific, Osterode am Harz, Germany). The pellet was fixed in 2.5% glutaraldehyde (16220, Electron Microscopy Sciences, Hatfield, PA, USA)/cacodylate buffer (0.1 mol l^{-1}, pH 7.2; 11650, Electron Microscopy Sciences), at room temperature for 1 h, then washed in cacodylate buffer for a further 30 min. The samples were postfixed in 1% osmium tetroxide (19150, Electron Microscopy Science) for 1 h at room temperature, then dehydrated through graded alcohol series (20821.296, VWR Chemicals, Radnor, PA, USA), and embedded in Epon 812 resin (45345, Sigma-Aldrich). Ultrathin sections of 80 nm were cut using Leica Ultracut UCT Ultramicrotome (Leica Biosystems, Wetzlar, Germany), contrasted with uranyl acetate and examined at 120 kV with a JSM-4000 electron microscope (JEOL, Tokyo, Japan). Images were captured digitally by an Orius 1000 camera (Gatan, Abingdon, United Kingdom).

Statistical analyses

GraphPad Prism Software (GraphPad Software, Inc., San Diego, CA, USA) was used to conduct statistical analyses. Two-tailed Student's *t*-test

[Downloaded free from http://www.ajandrology.com on Thursday, July 9, 2020, IP: 92.167.220.122]

for unpaired data was used to evaluate single comparisons between different experimental groups, which exhibited Gaussian distribution as checked by Shapiro–Wilk normality test using GraphPad Prism Software. Differences were considered statistically significant for a value of $P < 0.05$.

RESULTS

Clinical data

Ten cryptorchid patients attending the Laboratory of Reproductive Biology CECOS (University Hospital Center of Rennes, France) for assisted reproduction technology and eight normozoospermic individuals before vasectomy were enrolled in this study. The results from clinical analysis are summarized in **Table 1**. The data show a strong decrease of semen parameters (concentration, mobility, and the percentage of normal forms of spermatozoa) in men with cryptorchid history.

Immunolocalization of autophagy-related proteins in spermatozoa from cryptorchid and control patients

To assess the autophagy status in cryptorchid spermatozoa, we analyzed the immunodistribution of autophagy proteins which are specific markers of different stages of autophagy in comparison with the control samples.

In both normal and cryptorchid spermatozoa, the early autophagy marker ATG9 protein was mainly detected in the sperm head, namely, in its apical region (**Figure 1**). Isolated anti-ATG9 points were also detected in the spermatozoon neck, probably in association with the basal body (**Figure 1a**, inset 1, arrowhead). In some spermatozoa from both normal and cryptorchid patients, a very strong anti-ATG9 immunoreactivity was noticed in the sperm head equatorial segment, whereas the apical region was almost free of anti-ATG9 immunostaining (**Figure 1a,** inset 2; **Figure 1b**, inset 2). In control preparations (treatment of samples with primary antibody preincubated with ATG9 blocking peptide), only a faint homogenous green staining was observed in both spermatozoon head and tail (**Figure 1c**). We divided the ATG9 staining profiles in the specimens from control and cryptorchid patients into two types (type 1 and type 2; **Figure 1** legend). Statistical analysis did not reveal significant difference in the repartition of ATG9 staining profiles between both groups analyzed (**Figure 1d**).

The immunolocalization of the autophagosome marker LC3 protein was not the same as that of ATG9. In control spermatozoa, the anti-LC3 immunostaining was detected in the acrosome and in the midpiece of the tail (**Figure 2a**). In some cases, faint immunostaining was also detected in the flagellum (**Figure 2a**). Some spermatozoa from normozoospermic patients also exhibited a strong anti-LC3 immunoreactivity in the sperm head equatorial segment (**Figure 2a**, arrow). In spermatozoa from men with cryptorchid history, anti-LC3 immunoreactivity was more pronounced compared to the control. The strongest anti-LC3 immunoreactivity was detected in the spermatozoon tail. Indeed, the neck and the midpiece were strongly stained with anti-LC3 antibodies (**Figure 2b**). Of note is that both the axial filament and the end piece of the flagellum were also stained with anti-LC3 antibodies. We divided LC3 staining profiles in the specimens from control and cryptorchid spermatozoa into two types (type 1 and type 2; **Figure 2** legend). In type 1 spermatozoa, a faint anti-LC3 immunostaining was detected in spermatozoa head and tail, including axial filament, whereas in type 2 spermatozoa, anti-LC3 immunostaining was present in the equatorial segment, in the acrosome and in the midpiece of the tail. Control experiments using LC-3 blocking peptide demonstrated the specificity of LC-3 staining (**Figure 2c**). Statistical analysis revealed the quasi-equivalence of type 1 and type 2 LC3-immunodistribution in cryptorchid patients compared to the control, in which the type 2 immunodistribution was prevalent (**Figure 2d**).

In control specimens, immunostaining against autophagy substrate p62 protein was detected in the postacrosomal region of the spermatozoa and in the midpiece of the tail (**Figure 2e**). No specific anti-p62 immunostaining was detected in sperm cells from the patients with cryptorchid history (**Figure 2f**). Control experiments using rabbit non-immune serum demonstrated the specificity of p62 staining (**Figure 2g**). Only rare spermatozoa from cryptorchid patients presented a faint anti-p62 immunostaining (**Figure 2f** and **2h**).

Table 1: Semen parameter values (mean±standard error) of men with cryptorchid history and fertile control

Variables	*Cryptorchid history (n=10)*	*Control (n=8)*
Age (year)	34.5±1.6	33.5±2.3
Volume of ejaculate (ml)	2.5±0.4	3.6±0.3
Sperm concentration (10^6 ml^{-1})	<0.1	90.5±17.8
Motility (%)	10.0±5.7	53.5±3.8
Morphology (percentage of normal forms, %)	ND[a]	48.2±3.9
Cryptorchid's laterality (unilateral/bilateral)	5/5	0

[a]According to David classification. ND: not determined (data are missing about morphology of cryptorchid spermatozoa because they were rare)

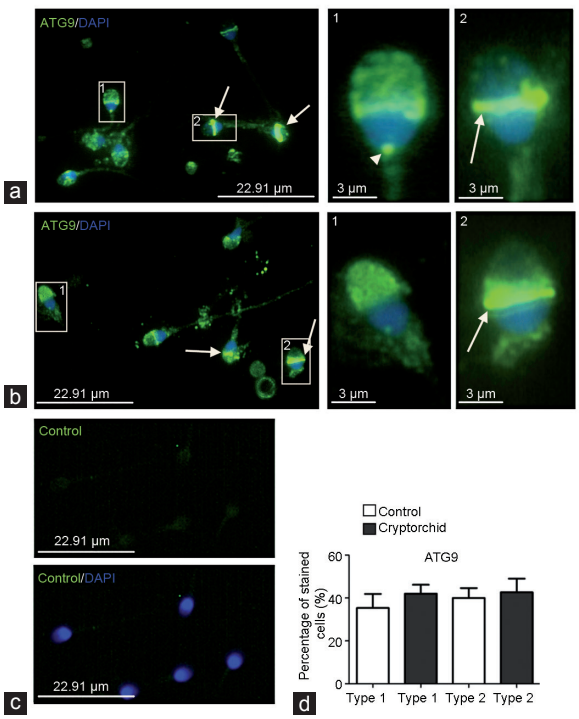


Figure 1: Immunodistribution of ATG9 protein in spermatozoa from (**a**) normal and (**b**) cryptorchid patients. IF analysis shows anti-ATG9 staining (green) in apical region of sperm head (type 1 staining), spermatozoon neck (arrowhead) and sperm head equatorial segment (type 2 staining, arrow). The pictures were merged with DAPI-stained nuclei (blue). 1 and 2 are higher magnifications of fragments from **a** and **b**. (**c**) A control specimen treated with the primary antibody preincubated with corresponding blocking peptide (see Patients and Methods; upper panel). Bottom panel is the merge with DAPI-stained nuclei. All pictures in **a**, **b**, and **c** were taken at the same exposition time. (**d**) Histogram showing the relative quantity of type 1 and type 2 spermatozoa in the preparations from normal and cryptorchid patients. ATG9: autophagy-related 9; IF: immunofluorescence; DAPI: 4,6-diaminido-2-phenylindole.

[Downloaded free from http://www.ajandrology.com on Thursday, July 9, 2020, IP: 92.167.220.122]

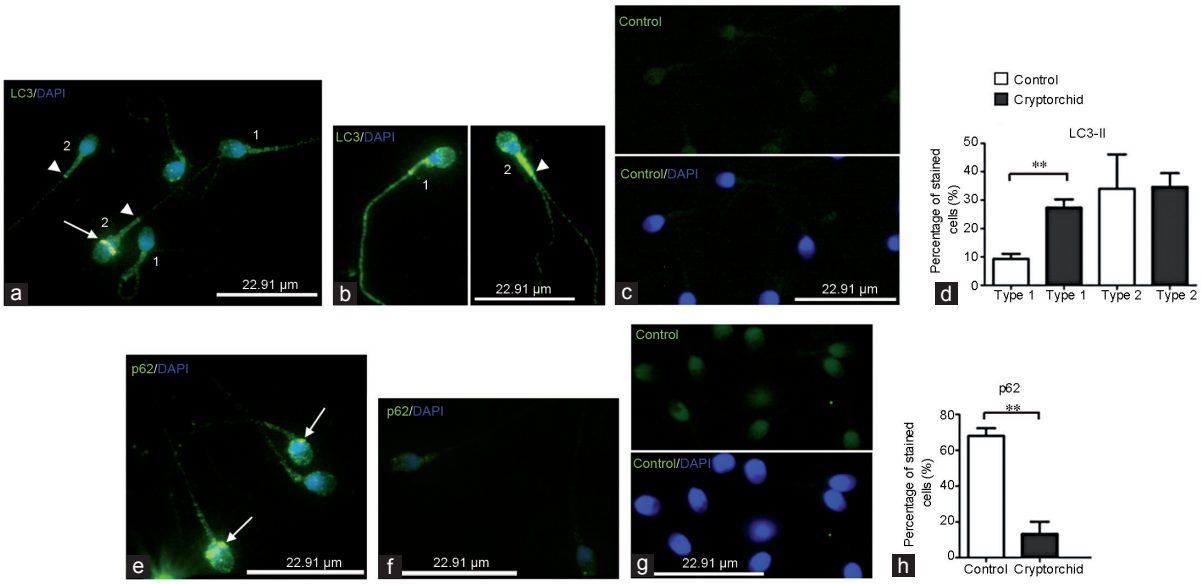


Figure 2: Immunodistribution of LC3 and p62 proteins in spermatozoa from normal and cryptorchid patients. (**a**) Faint anti-LC3 immunoreactivity (green) is detected in spermatozoa head and tail including axial filament (type 1 staining); in head equatorial segment (arrow), acrosome and the midpiece of the tail (type 2 staining). Note no staining in the axial filament and the end piece of flagellum in type 2 spermatozoa (arrowhead). (**b**) Pronounced anti-LC3 immunostaining is detected in acrosome and along the tail of cryptorchid spermatozoa including axial filament and end piece of flagellum (type 1 staining); very strong anti-LC3 immunostaining is present in the midpiece (**b**, arrowhead), but not in the axial filament in type 2 spermatozoa. (**c**) A control specimen treated with the primary antibody preincubated with LC3-blocking peptide (see Patients and Methods; upper panel). Bottom panel is the merge with DAPI-stained nuclei. (**d**) Histogram showing the relative quantity of type 1 and type 2 spermatozoa in the preparations from normal and cryptorchid patients. (**e**) Postacrosomal region (arrow) of control spermatozoa and the midpiece of the tail were stained with anti-p62 antibodies. (**f**) Anti-p62 immunostaining in cryptorchid spermatozoa. (**g**) Control specimen incubated with nonimmune rabbit serum instead of the primary antibody (upper panel). Bottom panel is the merge with DAPI-stained nuclei. (**h**) Histogram showing the relative quantity of spermatozoa stained with anti-p62 antibodies in the preparations from normal and cryptorchid patients. $^{**}P<0.05$. LC3: microtubule-associated protein, 1A/1B-light chain 3; DAPI: 4,6- diaminido-2-phenylindole.

Thus, the distribution of several autophagy-related proteins in cryptorchid spermatozoa shows a deviation compared to the control. To confirm our immunocytochemistry results, we carried out a TEM analysis to compare spermatozoa from control and from patients.

TEM analysis of spermatozoa from cryptorchid and control patients

TEM analysis revealed numerous morphological abnormalities in sperm samples from cryptorchid patients. Immature forms of spermatozoa were extremely frequent in those specimens. Immature cells were recognized by misshapen, round or elliptic nuclei with uncondensed chromatin, large cytoplasmic droplets, coiled altered axonemes, and aberrant acrosomes (**Figure 3** and **4**).

The midpiece of cryptorchid spermatozoa did not present regularly arranged mitochondria. While in control specimens, mitochondria were approximately equal in size and regularly arranged (**Figure 3a**), in cryptorchid specimens they had a more disordered arrangement and showed more variation in size (**Figure 3b–3e**). In rare cases, acephalic spermatozoa with abnormally large mitochondria were also detected (**Figure 3d**). In contrast to control (**Figure 3a**), in cryptorchid sperm, a large body of mitochondria were scattered in cytoplasmic droplets without forming the gyres around the axoneme (**Figure 3b–3d**). The asymmetry of mitochondrial gyres with an increased number of mitochondria was also detected (**Figure 3e**). In overall, mitochondria from patients with cryptorchid history often looked swollen (**Figure 3d**) and partly disorganized (**Figure 3b** and **3c**) compared to the control (**Figure 3a**).

We often detected double-membrane-limited vacuoles in large cytoplasmic droplet in cryptorchid spermatozoa, close to disorganized mitochondrial gyres (**Figure 4a** and **4b**). By morphological criteria, these vacuoles corresponded to autophagosome vesicles. We also detected autophagosomes in close proximity to aberrant nuclei in sections passing through postequatorial segments of sperm head (**Figure 4c** and **4e**). The content of autophagic vacuoles was heterogeneous, so that some of these vacuoles were filled with partly degraded vesicular material (**Figure 4b–4d**), others contained the remnants of mitochondria (**Figure 4e** and **4f**). On the contrary, we never observed double-membrane-limited autophagosome vesicles in the sperm cells from control patients.

Collectively, TEM data are in agreement with immunofluorescence (IF) analysis, manifesting activation of autophagy in cryptorchid spermatozoa. To our knowledge, we reveal for the first time the presence of autophagosomes filled with heterogeneous content in human cryptorchid spermatozoa.

DISCUSSION

Here, we show for the first time an increased status of autophagy in sperm cells from cryptorchid patients, probably related to testis hyperthermic conditions. Autophagy is involved in spermatogenesis.[35–37] Autophagosomes are detected in cultured rat spermatocytes.[38] In mouse germ cells, heat stress induces autophagy in addition to apoptosis.[39] Moreover, exposition of ejaculates to elevated temperature also increases autophagy in human sperm.[40]

In the present study, the activation of autophagy in the cryptorchid sperm was demonstrated by IF and TEM experiments. Using antibodies against the main autophagy membrane protein LC3-II, we revealed a pronounced immunostaining in the midpiece of the tail in cryptorchid sperm compared to control. Such strong anti-LC3 immunostaining in

[Downloaded free from http://www.ajandrology.com on Thursday, July 9, 2020, IP: 92.167.220.122]

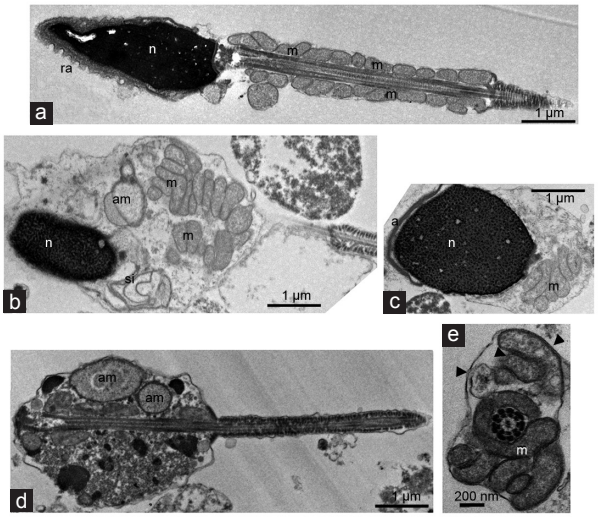


Figure 3: Transmission electron microscopy analysis of normal and cryptorchid spermatozoa. (**a**) Longitudinal section of spermatozoa from control man presents 13–14 mitochondrial gyres in a regular arrangement. Longitudinal sections of spermatozoa from cryptorchid men manifesting (**b** and **c**) partly packaged, (**d**) unpackaged mitochondrial gyres and (**b** and **d**) aberrant mitochondria in large cytoplasmic droplet. Note the nuclei with an uncondensed chromatin in **b** and **c**, (**c**) partly detached nuclear envelope (asterisk), or (**b**) those (arrow) forming swirling invaginations into the cytoplasm, and (**d**) seemingly acephalic spermatozoon. (**e**) Cross-section passing through the connecting piece/midpiece of spermatozoon reveals both intact and damaged mitochondria (arrowhead) gyred around the correct axoneme. a: acrosome; ra: reacted acrosome; m: mitochondria; am: aberrant mitochondria; n: nucleus; si: swirling invaginations.

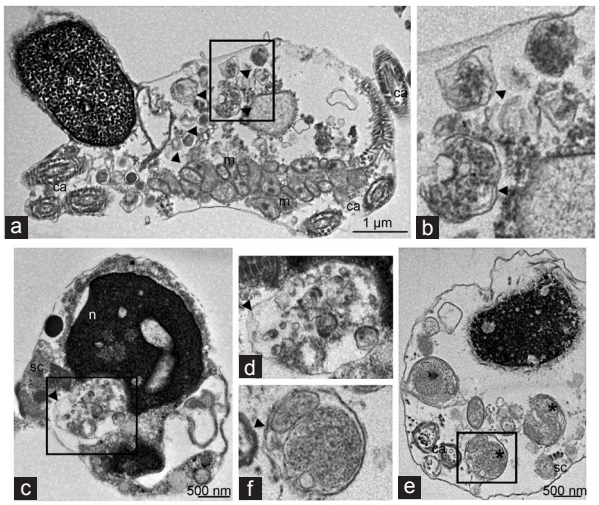


Figure 4: Transmission electron microscopy analysis of cryptorchid spermatozoa reveals autophagic vacuoles. (**a**) Longitudinal section of cryptorchid spermatozoon, exhibiting the nucleus with uncondensed chromatin, partly detached nuclear envelope (arrow), and coiled axoneme (ca). The large cytoplasmic droplet contains the autophagic vacuoles (arrowheads), located next to irregular gyres of damaged mitochondria (m). (**b**) A higher magnification of the selected area from **a**. Note double membrane-limited autophagic vesicles (arrowheads) containing partly degraded vesicular material. Cross-sections of cryptorchid spermatozoa pass through the postequatorial segment of the heads, which manifest (**c**) chromatin rarefaction and (**e**) granulation. (**e**) Coiled aberrant axonemes (ca) and the fragments of segmented columns (sc) forming conico-cylindrical sleeve are scattered in the cytoplasm. (**d**) Double-membrane-limited autophagosomes (arrowheads) filled with vesicular material locate in close proximity to (**c**) the nucleus, (**e**) while partly degraded mitochondria (asterisk) are next to plasma membrane and seemingly fusion with it. **d** and **f** are higher magnifications from selected area from **c** and **e**, respectively showing (**d**) double membrane-limited autophagosomes (arrowhead) enclosing vesicles or (**f**) mitochondria. m: mitochondria; n: nucleus.

sperm tail midpiece was also reported after the treatment of ejaculates from normozoospermic patients with bafilomicin A, a drug currently used to assess autophagic flux.[40] Anti-LC3 immunoreactivity was also observed in the acrosome and in the equatorial segment in both patient and control sperms. These data were confirmed by TEM analysis, which discerned numerous double-membrane-limited vacuoles, filled with heterogeneous contents in cryptorchid sperm. Autophagic vacuoles were detected not only in sperm tail midpiece, but also in the sperm head and in cytoplasmic droplets, which were often present in cryptorchid specimens. Of note, no autophagic vacuole was observed in sperm cells from normozoospermic controls. The presence of anti-LC3 immunostaining detected in the acrosome of control specimens could be due to the soluble form of LC3 protein, which is not associated with autophagic vesicles.[19]

Remarkably, the most frequent cargoes enclosed into the autophagosomes from cryptorchid sperm contained partly degraded mitochondria. This attests to the activation of mitophagy – a sort of selective autophagy which specifically targets the aberrant and damaged mitochondria.[41] The p62 protein is a specific adaptor in autophagy/mitophagy;[42] it accumulates when autophagy is inhibited, whereas it is degraded when autophagy is induced.[40] Thus, the undetectable level of p62 in cryptorchid sperm is in good agreement with TEM observations revealing the strong signs of autophagy/mitophagy in cryptorchid specimens.

Increased mitophagy implies a mitochondrial damage in cryptorchid sperm. It agrees with our TEM data, which unveil numerous abnormalities in sperm cell mitochondria. As usual, mitochondria from cryptorchid sperm appear swollen and partly disorganized compared to control ones. Besides, the abnormal assembly of mitochondria around the axoneme, and the asymmetry of mitochondrial gyres were observed (**Figure 3b** and **3e**). Our finding corroborates the study of seminal plasma from cryptorchid stallion,[43] in which abnormal mitochondria were also frequent in sperm cells. Together, these data suggest that sperm mitochondria are particularly vulnerable in cryptorchidism, being the substrate for autophagic degradation.

Because hyperthermic environment in body cavity is considered as the primary factor affecting spermatogenesis in cryptorchid testes,[30–32] its involvement in mitochondrial damage seems likely. We found no literature information on the temperature resistance of sperm mitochondria. Nevertheless, hyperthermia impairs heart mitochondria, leading to the generation of reactive oxygen species (ROS) in mitochondrial matrix[44] and mitochondrial membrane damage. Interestingly, autophagic vacuoles containing damaged mitochondria have been found in germ cells from heat stressed mouse testes.[39] Data from adipose tissue also support the involvement of mitophagy in regulation of mitochondrial homeostasis during temperature challenge.[45] Thus, the abnormal temperature environment should be among the factors inducing mitochondrial damage and the activation of mitophagy in cryptorchid sperm. Besides, impaired mitochondrial integrity we detected in cryptorchid samples could be related to epididymis anomalies. Indeed, maturation and modification of the outer mitochondrial membrane occur during sperm transit through epididymis; the failure of this process results in asthenozoospermia.[46] Because cryptorchidism is associated with epididymis anomalies,[13,47]

[Downloaded free from http://www.ajandrology.com on Thursday, July 9, 2020, IP: 92.167.220.122]

this could provoke the aberrations in mitochondrial structure and integrity we detected by TEM.

Mitochondria are the main source of sperm-produced reactive oxygen species (ROS), which can cause oxidative damage, if produced in an unchecked manner.[48,49] Remarkably, ROS is known to activate autophagy *in vitro*.[50] ROS have a pathological effect on male gametes resulting in apoptosis-like phenomenon.[49,51] Swollen mitochondria are one of the hallmarks of early apoptosis stages in cells,[52] and the disruption of mitochondrial membrane facilitates the release of cytochrome c in cell cytoplasm triggering intrinsic mitochondria-mediated apoptosis.[53]

Mitochondria are considered as a switch between apoptosis and autophagy.[54] Indeed, if the damaged mitochondria are not removed by mitophagy, both membrane potential loss and cytochrome c release can trigger apoptosis.[54] By this way, autophagy counteracts apoptosis, contributing to cell survival. Interestingly, our TEM data did not reveal the signs of late stage apoptotic process, characterized by strongly marginated chromatin[55] in cryptorchid specimens. High incidence of autophagosomes filled with swollen mitochondria implies the involvement of autophagy in the survival of cryptorchid sperm cells.

The defects in sperm mitochondrial ultrastructure[49] are associated with decreased sperm motility in humans.[56,57] This is in agreement with data from this study, because samples from cryptorchid patients exhibited very poor motility compared to the control (**Table 1**). Remarkably, autophagy has been recently demonstrated to influence sperm motility as well. Thus, sperm cells treated with autophagy activators exhibited an increased motility, whereas treatment with autophagy blockers decreased their motility.[40] Therefore, the increased autophagy could be important for maintaining the motility of cryptorchid sperm, even if it remains very poor.

In agreement with literature data,[17,58] our TEM observations also detected a large amount of immature sperm cells with uncondensed chromatin, large cytoplasmic residues, which sometimes contained an altered axoneme in the specimens from cryptorchid patients. The loss of the majority of the cytoplasm occurs during spermiogenesis concomitantly with the loss of excessive mitochondria inside the residual bodies.[56] As recently demonstrated using *ATG7* knock-out mice, this process is tightly regulated by autophagy.[24] Besides, the involvement of autophagy in the elimination of excessive mitochondria was recently demonstrated during gametogenesis in fish.[37] Thus, the presence of autophagosomes with the remnants of mitochondria in cytoplasmic residues might also be interpreted as a lack of timely maturation of cryptorchid sperm.

Collectively, the sperm cells from cryptorchid patients exhibit strong signs of autophagy activation. While aberrant mitochondria were the most frequent cargoes in autophagic vacuoles, the presence of other cargoes inside the autophagosomes indicates the general pattern of activation of degradative autophagy. This may have a positive role in the physiology of cryptorchid sperm, contributing to its viability and motility.

AUTHORS CONTRIBUTIONS

MGY carried out study design, execution, analysis of data, and writing/revising the manuscript. A Buschiazzo participated in immunohistochemistry and electron microscopy experiments, analysis of data, and manuscript writing. A Burel and MTL participated in electron microscopy experiments. CP, GJ, and S J recruited the patients and controls, and performed sperm and genetic analysis. BJ participated in study conception and manuscript revision. NB was involved in study conception, data analysis, and manuscript revision. CR is the senior author involved in study conception, data analysis, and manuscript revision. All authors read and approved the final manuscript.

COMPETING INTERESTS

All authors declare no competing interests.

ACKNOWLEDGMENTS

We thank Prof. V Catros and Dr. JC Hervé for critical reading of the manuscript. We thank H2P2 platform and MRIC platform from Rennes University. MGY was welcomed as invited researcher and invited Professor by Universite de Rennes1, CHU de Rennes and INSERM IRSET U 1085. MGY acknowledges the DRC (Direction de la Recherche Clinique du CHU de Rennes). CR acknowledges financial support from Rennes Metropole (AIS 2015) and Agence de BioMédecine. This work was supported by funding from Universite de Rennes1, Institut National de la Santé et de la Recherche Médicale (INSERM) and CHU de Rennes.

REFERENCES

1 Virtanen HE, Bjerknes R, Cortes D, Jorgensen N, Rajpert-De Meyts E, *et al*. Cryptorchidism: classification, prevalence and long term consequences. *Acta Paediatr* 2007; 96: 611–6.
2 Niedzielski JK, Oszukowska E, Słowikowska-Hilczer J. Undescended testis – current trends and guidelines: a review of the literature. *Arch Med Sci* 2016; 12: 667–77.
3 Dada R, Gupta NP, Kucheria K. Case report: cryptorchidism and AZF microdeletion. *Asian J Androl* 2002; 4: 148.
4 Dohle GR, Colpi GM, Hargreave TB, Papp GK, Jungwirth A, *et al*. The EAU working group on male infertility. EAU guidelines on male infertility. *Eur Urol* 2005; 48: 703–11.
5 Ferguson L, Agoulnik AI. Testicular cancer and cryptorchidism. *Front Endocrinol (Lausanne)* 2013; 4: 32.
6 Gotoh M, Miyake K, Mitsuya H, Hoshino T, Yamada K. Cytoplasmic inclusion bodies in Leydig cells from the testes of postpubertal cryptorchid patients. *Int J Androl* 1983; 6: 221–8.
7 Murphy L, O'Shaughnessy PJ. Effect of cryptorchidism on testicular and Leydig cell androgen production in the mouse. *Int J Androl* 1991; 14: 66–74.
8 Rune GM, Mayr J, Neugebauer H, Anders C, Sauer H. Pattern of Sertoli cell degeneration in cryptorchid prepubertal testes. *Int J Androl* 1992; 15: 19–31.
9 Govender D, Sing Y, Chetty R. Sertoli cell nodules in the undescended testis: a histochemical, immunohistochemical, and ultrastructural study of hyaline deposits. *J Clin Pathol* 2004; 57: 802–6.
10 Chen J, Fok KL, Chen H, Zhang XH, Xu WM, *et al*. Cryptorchidism-induced CFTR downregulation results in disruption of testicular tight junctions through up-regulation of NF-κB/COX- 2/PGE2. *Hum Reprod* 2012; 27: 2585–97.
11 Moon JH, Yoo DY, Jo YK, Kim GA, Jung HY, *et al*. Unilateral cryptorchidism induces morphological changes of testes and hyperplasia of Sertoli cells in a dog. *Lab Anim Res* 2014; 30: 185–9.
12 Davis EL, Shpall RA, Goldstein AM, Morrow JW. Congenitally uncoiled epididymis in a cryptorchid testis. *J Urol* 1974; 111: 618–20.
13 Caterino S, Lorenzon L, Cavallini M, Cavaniglia D, Ferro F. Epididymal-testicular fusion anomalies in cryptorchidism are associated with proximal location of the undescended testis and with a widely patent processus vaginalis. *J Anat* 2014; 225: 473–8.
14 La Vignera S, Calogero AE, Condorelli R, Marziani A, Cannizzaro MA, *et al*. Cryptorchidism and its long-term complications. *Eur Rev Med Pharmacol Sci* 2009; 13: 351–6.
15 Hutson JM, Balic A, Nation T, Southwell B. Cryptorchidism. *Semin Pediatr Surg* 2010; 19: 215–24.
16 Hutson JM, Vikraman J, Li R, Thorup J. Undescended testis: what paediatricians need to know. *J Paediatr Child Health* 2017; 53: 1101–4.
17 Moretti E, Di Cairano G, Capitani S, Scapigliati G, Baccetti B, *et al*. Cryptorchidism and semen quality: a TEM and molecular study. *J Androl* 2007; 28: 194–9.
18 Lee PA, Coughlin MT. Fertility after bilateral cryptorchidism. Evaluation by paternity, hormone, and semen data. *Horm Res* 2001; 55: 28–32.
19 Feng Y, He D, Yao Z, Klionsky DJ. The machinery of macroautophagy. *Cell Res* 2014; 24: 24–41.
20 Ding WX, Yin XM. Mitophagy: mechanisms, pathophysiological roles, and analysis. *Biol Chem* 2012; 7: 547–64.
21 Ziegler U, Groscurth P. Morphological features of cell death. *News Physiol Sci* 2004; 19: 124–8.
22 Martinet W, Timmermans JP, De Meyer GR. Methods to assess autophagy *in situ* – transmission electron microscopy versus immunohistochemistry. *Methods Enzymol* 2014; 543: 89–114.
23 Wang H, Wan H, Li X, Liu W, Chen Q, *et al*. Atg7 is required for acrosome biogenesis during spermatogenesis in mice. *Cell Res* 2014; 24: 852–69.

[Downloaded free from http://www.ajandrology.com on Thursday, July 9, 2020, IP: 92.167.220.122]

24 Liu C, Wang H, Shang Y, Liu W, Song Z, *et al*. Autophagy is required for ectoplasmic specialization assembly in sertoli cells. *Autophagy* 2016; 12: 814–32.
25 Jegou B. The Sertoli-germ cell communication network in mammals. *Int Rev Cytol* 1993; 147: 25–96.
26 Cummins JM, Glover TD. Artificial cryptorchidism and fertility in the rabbit. *J Reprod Fertil* 1970; 23: 423–33.
27 Ploen LN, Hakarsson N. Abnormal epididymal spermatozoa two to thirty-five days after a brief experimental cryptorchidism in the rabbit. *Int J Androl* 1978; 1: 250–61.
28 Pinart E, Camps R, Briz MD, Bonet S, Egozcue J. Unilateral spontaneous abdominal cryptorchidism: structural and ultrastructural study of sperm morphology. *Anim Reprod Sci* 1998; 49: 247–68.
29 Zhang Y, Calderwood SK. Autophagy, protein aggregation and hyperthermia: a mini-review. *Int J Hyperthermia* 2011; 27: 409–14.
30 Kumagai J, Fukuda J, Kodama H, Murata M, Kawamura K, *et al*. Germ cell-specific heat shock protein 105 binds to p53 in a temperature-sensitive manner in rat testis. *Eur J Biochem* 2000; 267: 3073–8.
31 Yin J, Ni B, Tian ZQ, Yang F, Liao WG, *et al*. Regulatory effects of autophagy on spermatogenesis. *Biol Reprod* 2017; 96: 525–30.
32 Izu H, Inouye S, Fujimoto M, Shiraishi K, Naito K, *et al*. Heat shock transcription factor 1 is involved in quality-control mechanisms in male germ cells. *Biol Reprod* 2004; 70: 18–24.
33 Wei Y, Zhou Y, Tang XL, Liu B, Shen LJ, *et al*. Testicular developmental impairment caused by flutamide-induced and DEHP-induced cryptorchid rat models is mediated by excessive apoptosis and deficient autophagy. *Toxicol Mech Methods* 2018; 28: 507–19.
34 World Health Organization. WHO Laboratory Manual for the Examination and Processing of Human Semen. 5th ed. Geneva: World Health Organization; 2010.
35 Ozturk N, Steger K, Schagdarsurengin U. The impact of autophagy in spermiogenesis. *Asian J Androl* 2017; 19: 617–8.
36 Oliveira PF, Cheng CY, Alves MG. Emerging role for mammalian target of rapamycin in male fertility. *Trends Endocrinol Metab* 2017; 28: 165–7.
37 Herpin A, Englberger E, Zehner M, Wacker R, Gessler M, *et al*. Defective autophagy through *epg5* mutation results in failure to reduce germ plasm and mitochondria. *FASEB J* 2015; 29: 4145–61.
38 Bustamante-Marin X, Quiroga C, Lavandero S, Reyes JG, Moreno RD. Apoptosis, necrosis and autophagy are influenced by metabolic energy sources in cultured rat spermatocytes. *Apoptosis* 2012; 17: 539–50.
39 Zhang M, Jiang M, Bi Y, Zhu H, Zhou Z, *et al*. Autophagy and apoptosis act as partners to induce germ cell death after heat stress in mice. *PLoS One* 2012; 7: e41412.
40 Aparicio IM, Espino J, Bejarano I, Gallardo-Soler A, Campo ML, *et al*. Autophagy-related proteins are functionally active in human spermatozoa and may be involved in the regulation of cell survival and motility. *Sci Rep* 2016; 6: 33647.
41 Liu H, Dai C, Fan Y, Guo B, Ren K, *et al*. From autophagy to mitophagy: the roles of P62 in neurodegenerative diseases. *J Bioenerg Biomembr* 2017; 49: 413–22.
42 Chu CT. Mechanisms of selective autophagy and mitophagy: implications for neurodegenerative diseases. *Neurobiol Dis* 2019; 122: 23–34.
43 Ares MJ, Neck KE, Evans JW, Caceci T. Ultrastructural abnormalities in equine spermatozoa from a cryptorchid stallion. *J Equine Vet Sci* 1988; 8: 122–4.
44 Zukiene R, Nauciene Z, Ciapaite J, Mildaziene V. Acute temperature resistance threshold in heart mitochondria: febrile temperature activates function but exceeding it collapses the membrane barrier. *Int J Hyperthermia* 2010; 26: 56–66.
45 Lu Y, Fujioka H, Joshi D, Li Q, Sangwung P, *et al*. Mitophagy is required for brown adipose tissue mitochondrial homeostasis during cold challenge. *Sci Rep* 2018; 8: 8251.
46 Calvin HI, Bedford JM. Formation of disulphide bonds in the nucleus and accessory structures of mammalian spermatozoa during maturation in the epididymis. *J Reprod Fertil* 1971; 13 (Suppl 13) : 65–75.
47 Koff WJ, Scaletscky R. Malformations of the epididymis in undescended testis. *J Urol* 1990; 143: 340–3.
48 Schieber M, Chandel NS. ROS function in redox signaling and oxidative stress. *Curr Biol* 2014; 24: R453–62.
49 Amaral A, Lourenço B, Marques M, Ramalho-Santos J. Mitochondria functionality and sperm quality. *Reproduction* 2013; 146: R163–74.
50 Ding WX, Ni HM, Li M, Liao Y, Chen X, *et al*. Nix is critical to two distinct phases of mitophagy, reactive oxygen species-mediated autophagy induction and Parkin-ubiquitin-p62-mediated mitochondrial priming. *J Biol Chem* 2010; 285: 27879–90.
51 Amaral S, S Tavares R, Baptista M, Sousa MI, Silva A, *et al*. Mitochondrial functionality and chemical compound action on sperm function. *Curr Med Chem* 2016; 23: 3575–606.
52 Sesso A, Belizário JE, Marques MM, Higuchi ML, Schumacher RI, *et al*. Mitochondrial swelling and incipient outer membrane rupture in preapoptotic and apoptotic cells. *Anat Rec (Hoboken)* 2012; 295: 1647–59.
53 Wang C, Youle RJ. The role of mitochondria in apoptosis. *Annu Rev Genet* 2009; 43: 95–118.
54 Ferraro E, Cecconi F. Autophagic and apoptotic response to stress signals in mammalian cells. *Arch Biochem Biophys* 2007; 462: 210–9.
55 Baccetti B, Capitani S, Collodel G, Strehler E, Piomboni P. Recent advances in human sperm pathology. *Contraception* 2002; 65: 283–7.
56 Mundy AJ, Ryder TA, Edmonds DK. Asthenozoospermia and the human sperm mid-piece. *Hum Reprod* 1995; 10: 116–9.
57 Pelliccione F, Micillo A, Cordeschi G, D'Angeli A, Necozione S, *et al*. Altered ultrastructure of mitochondrial membranes is strongly associated with unexplained asthenozoospermia. *Fertil Steril* 2011; 95: 641–6.
58 Toppari J, Kaleva M. Maldescendus testis. *Horm Res* 1999; 51: 261-9.

This is an open access journal, and articles are distributed under the terms of the Creative Commons Attribution-NonCommercial-ShareAlike 4.0 License, which allows others to remix, tweak, and build upon the work non-commercially, as long as appropriate credit is given and the new creations are licensed under the identical terms.

©The Author(s)(2019)